Progress in Medical Devices
ISSN: 2957-5478

Zentime

Research Article https://doi.org/10.61189/017119gmeubf

# Detection of traumatic brain injury using eddy current damping technology

Wenjing Du, Rongguo Yan, Tingting Shi, Ke Wang, Shoucheng Chen

School of Health Science and Engineering, University of Shanghai for Science and Technology, Shanghai 200093, P. R. China.

**Corresponding author:** Rongguo Yan.

**Declaration of conflict of interest:** None.

Received February 21, 2025; Accepted April 16, 2025; Published December 31, 2025

## Highlights

- This paper presents a new method for brain injury detection, which uses eddy current damping technology. This method is more convenient and faster than the traditional detection method.
- This paper simulates the method in COMSOL software and then verifies it through experiments. The feasibility of the method is proved through the combination of simulation and experiments.

## Abstract

**Objectives:** To investigate the feasibility of using eddy current damping (ECD) technology as a portable and rapid alternative for detecting the location of cerebral hemorrhage. **Methods:** This study leveraged the significant conductivity difference between hemorrhagic and normal brain tissue. ECD technology involved the application of alternating current to a coil, generating a time-varying magnetic field that induces eddy currents in conductive tissues such as hemorrhagic regions. These eddy currents produced a secondary magnetic field that opposes the original, resulting in measurable changes in the ECD signal. Using COMSOL simulations, detailed models of the head, brain, hemorrhage, and coil were constructed to analyze electromagnetic coupling. Changes in coil resistance and inductance due to hemorrhagic tissue were quantified to evaluate the detectability of ECD signals. **Results:** Simulation results confirmed that cerebral hemorrhages generate measurable eddy current responses, which alter the resistance and inductance of the detection coil. These changes provide quantifiable ECD signals that can potentially indicate both the location and volume of hemorrhagic lesions. **Conclusions:** The findings demonstrate the feasibility of using ECD technology as a portable, rapid, and non-invasive method for detecting cerebral hemorrhage. Pending clinical validation, this approach could serve as a practical alternative to conventional imaging, particularly in emergency settings where speed and mobility are essential.

**Keywords:** Eddy current damping, traumatic brain injury, COMSOL multiphysics, finite element model of the human head

## Introduction

Traumatic brain injury (TBI) refers to damage to brain tissue caused by direct or indirect external force to the head and is classified as a mechanical injury. In clinical practice, TBI not only affects brain tissue but can also lead to dysfunction of the nervous and endocrine systems, resulting in complications such as limb impairment, cognitive decline, and psychological disorders [1]. Studies have shown that accurate assessment of TBI severity plays a crucial role in clinical decision-making. Early identification of the extent of brain injury and the location of intracranial hemorrhage (ICH) allows for timely and targeted treatment interventions [2]. Therefore, rapid and accurate assessment is essential to improving survival

**Address correspondence to: Rongguo Yan,** Department of Biomedical Engineering, School of Health Science and Engineering, University of Shanghai for Science and Technology, No. 516 Jungong Road, Yangpu, Shanghai 200093, P. R. China. E-mail: yanrongguo@usst.edu.cn.

rates and prognosis in patients with acute brain injuries.

Magnetic resonance imaging (MRI) and computed tomography (CT) are currently the most widely used imaging modalities for brain injury diagnosis [3]. MRI utilizes the hydrogen nucleus as the imaging basis, capitalizing on the varying water content across different tissues. These differences in hydrogen concentration result in distinct MRI signals, allowing differentiation between tissue types [4]. Brain injuries such as edema and hemorrhage alter the water content and thus can be detected using MRI [5]. However, MRI is contraindicated for patients with magnetic metal implants or pacemakers due to the presence of a strong magnetic field [6]. Additionally, MRI is time-consuming, generates significant acoustic noise, and produces large amounts of data, limiting its use in portable or emergency settings [7].

CT imaging works by scanning a specific area of the body with X-rays over a defined period [8]. The captured data is processed by a computer based on differences in tissue absorption and attenuation of X-rays [9]. This produces cross-sectional and 3D images that help identify pathological changes [10]. Despite its widespread clinical use, CT has several drawbacks. It relies on ionizing radiation, posing risks to certain populations, especially pregnant women [11]. Additionally, CT scanners are expensive, and the cost of each scan is relatively high. CT also has limitations in qualitative assessments [12]. More importantly, both CT and MRI lack portability and are unsuitable for time-critical situations [13]. For patients with acute brain injury, the time required to reach a hospital, undergo scanning, and receive a diagnosis may result in missed treatment windows, leading to adverse outcomes [14]. Thus, there is an urgent need for a portable device capable of quickly localizing intracranial injuries.

The basic principle of eddy current damping (ECD) technology is that when an alternating current is applied to a conductor, it generates a time-varying magnetic field, according to Ampère's law [15]. This changing magnetic field induces an electric field as described by Faraday's law of electromagnetic induction, generating circulating currents—known as eddy currents—within conductive materials [16]. These eddy currents, in turn, produce a secondary magnetic field that opposes the original one, resulting in a damping effect. Several international research institutions have explored the application of ECD in brain injury detection, demonstrating its feasibility through simulations, system prototyping, and experimental validation against conventional imaging techniques [17-19]. However, research in this area remains limited in China, and many existing simulation studies lack depth or precision.

In this study, we apply ECD technology to simulate brain injury detection using COMSOL Multiphysics. The basic concept involves generating a magnetic field from an alternating current (AC)-driven copper coil, with the brain modeled as a conductive medium. When this field interacts with hemorrhagic brain tissue, eddy currents are induced, leading to detectable changes in the coil's inductance and resistance. These changes are quantifiable and can be used to infer the injury's location. A simplified physical model of the human head was constructed, and sensor measurements confirmed that the equivalent resistance and inductance varied as expected in response to hemorrhagic lesions.

Compared with conventional imaging methods such as CT and MRI, this approach offers significant advantages. First, the portable design allows rapid detection in community clinics, at home, or even in pre-hospital emergency settings, breaking the reliance on fixed hospital equipment. Second, the electromagnetic-based detection system does not require expensive imaging devices or contrast agents, thereby reducing overall medical costs. These features highlight the high clinical value and potential of ECD technology for brain injury assessment.

## Materials and methods

### *COMSOL simulation*

#### *Theoretical analysis*

In the COMSOL Multiphysics environment, a numerical model was developed to simulate ECD for cerebral hemorrhage detection. An anatomically accurate head model was constructed and integrated with an electromagnetic coil. Tissue-specific bioelectromagnetic parameters were assigned to different anatomical regions. Finite element analysis was used to examine the spatial distribution and phase shift of eddy currents induced by the alternating magnetic field in hemorrhagic regions. Quantitative analysis of the perturbations in the electromagnetic field relative to hematoma volume confirmed the theoretical feasibility of ECD as a non-invasive method for detecting cerebral hemorrhage.

Normal brain tissue primarily consists of high-fat myelin, with a conductivity of approximately 0.2 S/m, while blood, rich in dissolved ions and charged proteins, has a conductivity of about 0.65 S/m [20]. Due to this significant difference, blood is considerably more conductive than brain tissue. When cerebral hemorrhage occurs, the localized change in conductivity leads to detectable eddy current phenomena under an applied magnetic field. These eddy currents generate secondary magnetic fields that oppose the original field, resulting in increased coil resistance and decreased inductance. By comparing the coil's resistance and inductance before and after measurement, the ECD signal can be quantified to identify the location of the hemorrhage.

Currently, magnetic scanners capable of operating at the micro-Tesla level are not widely used in clinical settings [21]. If it can be demonstrated that a magnetic field at this intensity induces a detectable eddy current in hemorrhagic tissue, it would support the feasibility of using ECD for precise localization of brain injuries at low field strengths.

The AC excitation frequency applied to the coil is set to 1 MHz. This frequency was selected based on several key considerations. First, the LDC1101 inductance-to-digital converter chip used in this study operates within the 500 kHz to 10 MHz range [19]. A frequency of 1 MHz lies near the midpoint of this range, allowing for stable and optimal performance. Furthermore, Shahristani et al. demonstrated that sensor coils resonate around 1 MHz when detecting brain tissue, suggesting this frequency aligns with the brain's natural electromagnetic resonance [19]. Operating at this resonant frequency maximizes the amplitude of the ECD signal, thereby improving detection sensitivity.

Second, the choice of frequency also balances two competing factors: spatial resolution and magnetic field penetration depth. Higher frequencies improve spatial resolution but reduce penetration, while lower frequencies allow deeper penetration at the cost of resolution. Through theoretical analysis and empirical validation, 1 MHz was found to provide an optimal trade-off between these parameters for cerebral hemorrhage detection.

In the simulation phase, the coil excitation current was set to 27 mA AC to ensure sufficient magnetic field intensity. For the physical experiment, however, power was supplied via a USB 2.0 interface, which allows a maximum current of 500 mA per port. To maintain a safe design margin and ensure stable operation, the experimental current was limited to 2.7 mA. This constraint was fully accounted for in the signal processing circuit design and component selection, ensuring system reliability and operational safety during real-time data acquisition and transmission.

*Model construction*

The simulation model was constructed using COMSOL Multiphysics. A realistic human head model was created using MRI coordinate files provided by the COMSOL library [22]. The model has an approximate height of 20 cm and width of 10 cm (**Figure 1A**). An ellipsoid (axes: 0.055 m, 0.065 m, 0.045 m) was inserted to represent the brain parenchyma, positioned at Y=-0.01 m and Z=0.07 m. A smaller ellipsoid (axes: 0.016 m, 0.018 m, 0.01 m) was added to simulate a cerebral hemorrhage, located at Y=-0.01 m and Z=0.1 m, ensuring it lies within the brain parenchyma (**Figure 1B**).

For the size and shape of the cerebral hemorrhage, the parameters were selected based on previous studies indicating that local brain stimulation may lead to an increase in local blood volume of approximately 1.5 mL. To enhance the accuracy of the COMSOL simulation, the modeled hemorrhage volume must closely approximate actual physiological values. Using a simplified formula for estimating intracerebral hemorrhage volume—defined as half the product of the three ellipsoidal semi-axes—the volume $V$ is calculated as:

$$V = \frac{a \times b \times c}{2} \tag{1}$$

Based on this formula, and the selected semi-axis lengths a, b, and c, the calculated volume of the ellipsoid is 1.44 mL. After iterative adjustments and validation in COMSOL, these dimensions were confirmed to yield a volume

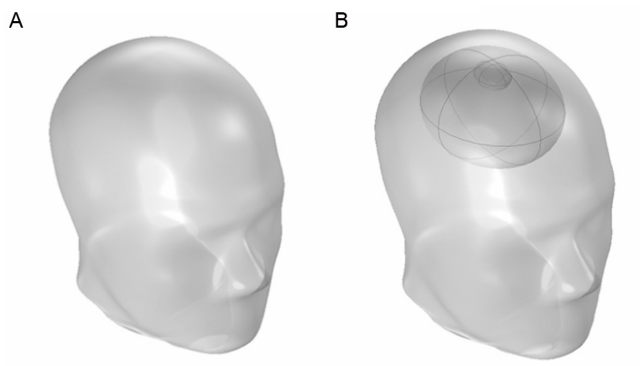


**Figure 1. Head model construction process.** (A) After the skull model lofting is completed. The Boolean operation segments the curve to ensure the successful lofting of the model, and the model generated after lofting is relatively smooth. (B) The brain parenchyma and cerebral hemorrhage models were constructed. It can be seen that the brain parenchyma and cerebral hemorrhage are in a reasonable position in the skull, with reasonable volume.

**Figure 2. The coil model is constructed.** The spatial position of the coil is above the overall model.

**Figure 3. The setting of coil current.** The red arrow represents the direction of the input current in the coil. In this direction, the magnetic field generated by the coil is downward to ensure that it can pass through the cerebral hemorrhage area.

closest to 1.5 mL, aligning with experimental requirements.

For the inductive coil design, a copper coil with an outer diameter of 8.8 cm is used in the simulation. The coil has the following parameters: a peak current of 2.7 mA, 6 turns, and a length of 6 cm. It is positioned directly above the head model, as shown in **Figure 2** [19].

Material parameters were assigned as follows:

Skull: conductivity 0.4 S/m, density 2000 kg/m$^3$, relative permittivity 827, relative permeability 1.

Brain parenchyma: conductivity 0.2 S/m, density 1000 kg/m$^3$, relative permittivity 827, relative permeability 1.

Cerebral hemorrhage: conductivity 0.65 S/m, density 1060 kg/m$^3$, relative permittivity 3030, relative permeability 1.

Coil (copper): conductivity 5.998 S/m, density 8960 kg/m$^3$, relative permittivity 1, relative permeability 1 [23].

These values simulate the physical properties of human tissues and the coil within the model.

The simulation involves applying alternating current to the coil to generate a magnetic field, which induces eddy currents in conductive tissue such as hemorrhagic areas. The magnetic field was modeled using the AC/DC module, focusing on flux density, current, inductance, and resistance. Ampère's law was used to define the magnetic field behavior, with magnetic insulation applied to all boundaries except where inapplicable. Initial values for the magnetic vector potential in x, y, and z directions were set to 0 Wb/m.

A uniform multi-turn coil was defined with numerical current excitation, and the direction of current input was aligned axially to ensure that the magnetic field penetrates downward

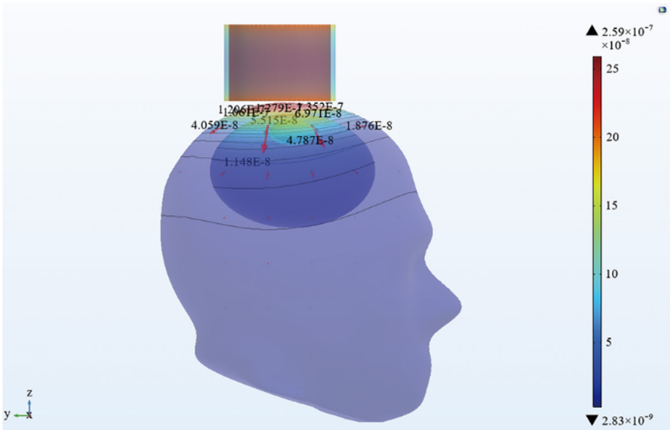


**Figure 4. Magnetic field distribution of the whole model.** The line on the model represents the magnetic field contour, and the number on the contour represents the value of the magnetic field on the contour. The red arrow represents the direction of the magnetic field. The larger the arrow, the stronger the magnetic field in this area.

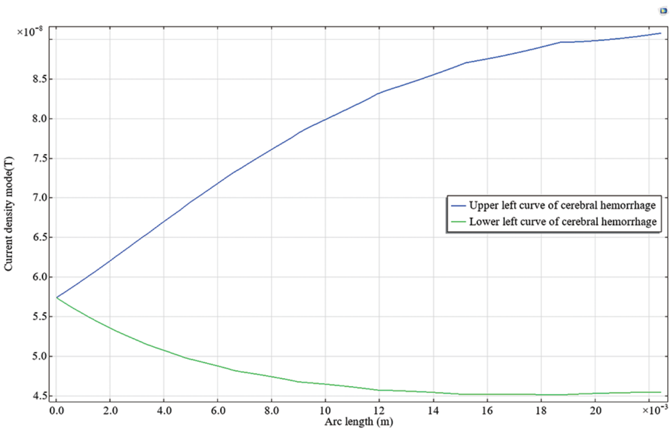


**Figure 5. The variation curve of magnetic flux density modulus with arc length in intracerebral hemorrhage.** The blue curve represents the upper left curve of cerebral hemorrhage, and the green curve represents the sitting curve of cerebral hemorrhage.

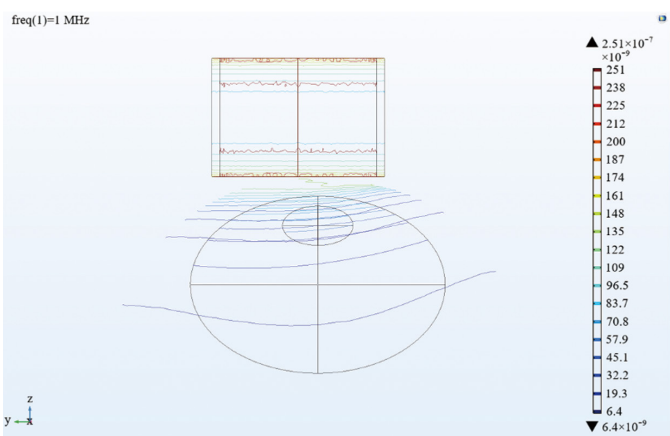


**Figure 6. Contour map of cerebral parenchyma and cerebral hemorrhage area.** The magnetic field generated by the coil can pass through the brain parenchyma and the area of cerebral hemorrhage.

through the hemorrhagic area (**Figure 3**). This completes the physical field setup for the magnetic field simulation.

*Simulation results*

To utilize ECD technology for precise localization of cerebral hemorrhage, it is essential to verify that the alternating magnetic field generated by the coil can penetrate the hemorrhagic area. This penetration induces eddy currents within the hemorrhage, enabling its localization. The simulated magnetic field distribution is shown in **Figure 4**. The red arrow indicates the direction of the magnetic field, which passes downward through the head. The contour lines reveal that the magnetic flux density near the hemorrhage is approximately $4.78 \times 10^{-8}$ T, confirming that the magnetic field effectively penetrates the hemorrhagic region.

To illustrate the spatial variation of magnetic flux density within the hemorrhagic area, two line plots were generated along different sagittal cross-sections. The x-axis represents arc length (m), and the y-axis shows magnetic flux density (T). As shown in **Figure 5**, the maximum flux density within the hemorrhage reaches $9.2 \times 10^{-8}$ T, while the lowest value, measured at the region furthest from the coil, is about $4.5 \times 10^{-8}$ T.

Additionally, a 3D visualization (**Figure 6**) was generated by adding contour lines and sectional views, illustrating the spatial distribution of the magnetic field. The contours clearly pass through the hemorrhagic region and gradually diminish in intensity with increasing distance from the coil. These visualizations confirm that the magnetic field is strong enough to reach the hemorrhagic site.

Once magnetic field penetration is confirmed, the next step is to detect hemorrhagic lesions by observing parameter changes in the coil. Eddy currents induced in the hemorrhagic region produce a secondary magnetic field that opposes the original field

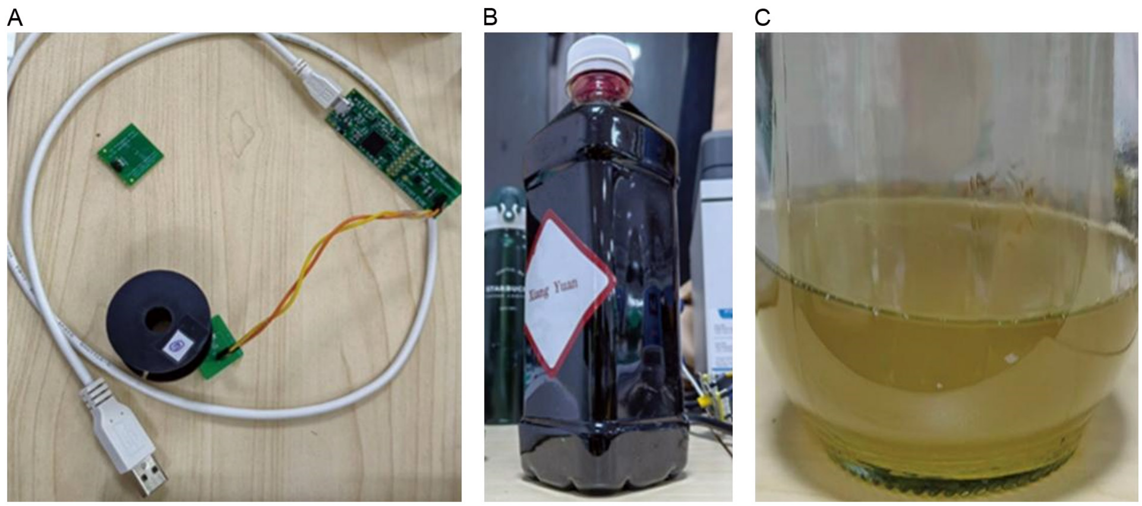


**Figure 7. Materials used in the experiment.** (A) The figure shows the coil sensor, processing circuit, and USB interface for data transmission with the computer. (B) Fresh pig blood. (C) Gelatin material.


**Figure 8. Magnetic field distribution cloud diagram of the whole model.**

from the coil. This interaction decreases the coil's inductance and increases its AC resistance due to energy loss. Therefore, variations in coil inductance and resistance can be used as indicators to detect cerebral hemorrhage.

*Experimental validation*

Simulation results suggest that hemorrhagic regions exhibit a damping effect on the coil's magnetic field, and that the field can effectively penetrate such regions. This forms the basis for quantifying ECD signals.

These signals can be measured using an LC resonant circuit, where a magnetic coil is coupled with a capacitor. The change in parallel resistance (Rp) of the system reflects variations in coil AC resistance. According to Equation (2):

$$Rp = \frac{L}{RC} \tag{2}$$

where Rp is the parallel resistance, L is inductance, R is resistance, and C is capacitance. This equation shows that Rp is inversely proportional to the AC resistance R. Hence, when the coil's AC resistance increases due to eddy current damping, the measured Rp decreases.

The experimental setup is shown in **Figure 7A**, and includes an inductive coil, oscillator, LDC1101 inductance-to-digital converter chip, and an MCU for data processing. Data are transmitted to a computer via USB, where inductance and resistance values are displayed in real time.

**Figure 7B** shows the fresh pig blood used in the experiment, and **Figure 7C** shows the gelatin phantom (conductivity: 0.2 S/m) used to simulate brain parenchyma. The experiment was conducted at room temperature and initiated immediately after gelatin solidification to prevent dissolution. A 10 mL volume of pig blood was injected into the gelatin to simulate a cerebral hemorrhage. The inductive coil was gradually brought closer to the phantom, and changes in inductance and resistance were monitored in real time via the host computer interface to evaluate detectability.

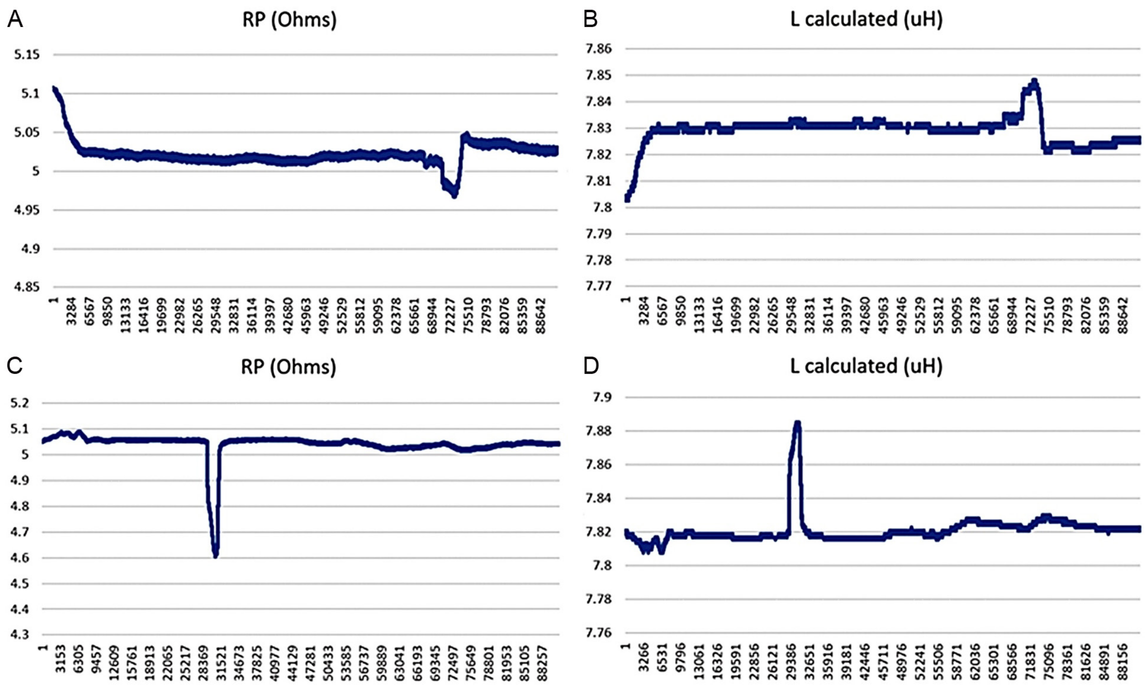


**Figure 9. The change curves of circuit resistance and inductance are obtained by the upper computer.** (A and B) The volume of pig blood is 40 ml. (C and D) The volume of pig blood is 60 ml.

## Results

The magnetic field contour plots of the simulation model confirm that the field generated by the coil can penetrate the cerebral hemorrhagic region, inducing eddy currents that produce a damping effect, thereby influencing the coil's electromagnetic characteristics. **Figure 8** illustrates the magnetic field distribution from the simulation results.

To assess the impact of hemorrhage on coil parameters, a reference model consisting only of the coil and air domain was established, keeping other boundary conditions constant. By comparing the inductance and AC resistance values between the two models, we observed a decrease in inductance and an increase in resistance in the presence of hemorrhage. These trends validate the feasibility of using ECD technology for detecting cerebral hemorrhage.

**Figure 9** presents experimental data collected on a computer. **Figure 9A** and **9B** display changes in resistance and inductance when 40 mL of pig blood is used as the detection target, while **Figure 9C** and **9D** show the corresponding data for 60 mL. The curves indicate that, as the detection probe approaches the blood sample, the resistance increases and the inductance decreases—consistent with ECD principles.

## Discussion

A variety of techniques have been explored for brain injury detection, including microwave imaging, volume impedance phase shift spectroscopy, near-infrared spectroscopy, EEG, transcranial Doppler ultrasound, and ECD [3, 24]. Among these, ECD stands out for its short detection time and high accuracy.

Given the importance of detecting changes in coil impedance caused by cerebral hemorrhage, a simplified coil-only model was constructed in COMSOL. This allowed for clear visualization of resistance and inductance changes under different conditions. **Figure 10** presents the coil-only model, and **Figure 11** shows the magnetic field distribution generated by the coil. The arrows indicate the magnetic field direction, while the color map reflects its magnitude.

In the coil-only model, the measured inductance is 2.4293±0.0015 μH, while in the full model (including the head), it decreases slightly to 2.4273±0.0018 μH. Meanwhile, the AC resistance increases from 2.12±0.05 mΩ (pure coil)


**Figure 10. The model with only coil and air domain.**

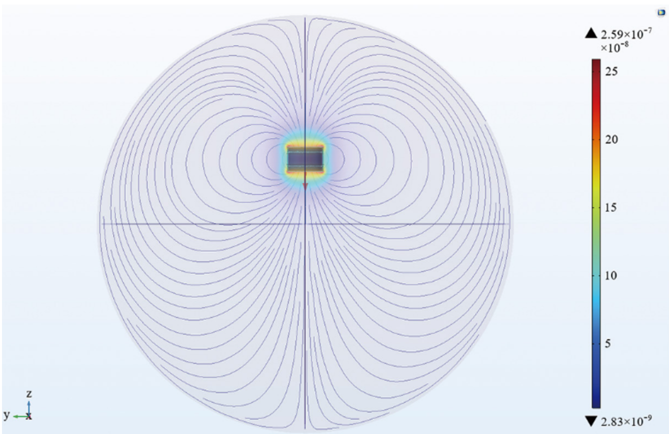


**Figure 11. Magnetic field distribution with coil model only.** The streamline represents the distribution of the magnetic field in the air domain.

to 3.19±0.07 mΩ (full model). These measurements account for an estimated ±0.5% instrument error and ±0.1% environmental variation. The observed decrease in inductance and increase in resistance support the predicted ECD effects.

This study integrates COMSOL simulations and experimental validation to assess the feasibility of ECD-based detection of cerebral hemorrhage. The electromagnetic model, which incorporates brain tissue and hemorrhagic regions, demonstrates that eddy currents generated in hemorrhagic areas affect coil impedance. Experiments using pig blood and custom detection circuitry revealed a significant correlation between blood volume and coil parameters, aligning with simulation predictions.

Although the current model assumes uniform brain tissue conductivity—neglecting regional (e.g., gray vs. white matter) and temporal variations that may affect quantitative accuracy—the consistent simulation and experimental trends confirm the fundamental feasibility of this approach. Future research will improve model accuracy by integrating tissue-specific conductivity and constructing multi-layered phantoms to better simulate brain structures. These results provide foundational evidence supporting the potential clinical application of ECD technology.

## Conclusion

This study uses finite element simulations in COMSOL to verify the feasibility of detecting cerebral hemorrhage via ECD technology. Simulation analysis demonstrates that hemorrhagic regions affect coil inductance and resistance, supporting the use of ECD for detection. A physical model was constructed, and experimental tests using a coil sensor confirmed that inductance and resistance change as expected in the presence of hemorrhage.

Since these changes are numerical differences, they are necessarily influenced by parameters such as hemorrhage volume and distance between the coil and hemorrhagic site. Therefore, this method enables qualitative assessment of hemorrhage by quantifying impedance changes.

Future efforts will aim to further quantify ECD signals induced by cerebral hemorrhage by analyzing precise changes in coil impedance. Optimizing coil geometry and parameters will also be explored to enhance detection performance. If cerebral hemorrhage volume and location can be accurately measured using ECD sensors, this technology could complement or even provide an alternative to current imaging modalities such as CT and MRI. ECD offers a fast, portable, and potentially cost-effective method for detecting intracerebral hemorrhage, overcoming the limitations of conventional techniques. We anticipate continued validation and refinement of this method in future studies.

**Author contributions:** Wenjing Du performed the data analyses and wrote the manuscript. Wenjing Du and Tingting Shi performed the experiment. Wenjing Du, Tingting Shi, Ke Wang, Shoucheng Chen and Rongguo Yan contributed significantly to the analysis and manuscript preparation.

## References

[1] Ghajar J. Traumatic brain injury. Lancet 2000; 356(9233):923-929.

[2] Maas AIR, Menon DK, Manley GT, et al. Traumatic brain injury: progress and challenges in prevention, clinical care, and research. Lancet Neurol 2022;21(11):1004-1060.

[3] Krausz AD, Korley FK, Burns MA. The Current State of Traumatic Brain Injury Biomarker Measurement Methods. Biosensors (Basel) 2021; 11(9):319.

[4] Kessler BA, Goh JL, Pajer HB, et al. Rapid-sequence MRI for evaluation of pediatric traumatic brain injury: a systematic review. J Neurosurg Pediatr 2021;28(3):278-286.

[5] Lunkova E, Guberman GI, Ptito A, et al. Noninvasive magnetic resonance imaging techniques in mild traumatic brain injury research and diagnosis. Hum Brain Mapp 2021;42(16): 5477-5494.

[6] Wald LL, McDaniel PC, Witzel T, et al. Low-cost and portable MRI. J Magn Reson Imaging 2020;52(3):686-696.

[7] Yang RJ, Yan HL, Han DM. Diagnostic Value of Brain Imaging of Multi Slice Spiral CT and MRI Examination for Cerebrovascular Diseases. Chinese Journal of CT and MRI 2021;19(7):15-17.

[8] Wang J, Hu Y, Wu P. Risk factors for positive brain CT scan in children with traumatic brain injury and GCS = 15: A retrospective study. Medicine (Baltimore) 2021;100(4):e24543.

[9] Moen TR, Chen B, Holmes DR 3rd, et al. Low-dose CT image and projection dataset. Med Phys 2021;48(2):902-911.

[10] Aide N, Lasnon C, Desmonts C, et al. Advances in PET/CT technology: an update. Semin Nucl Med 2022;52(3):286-301.

[11] Rehani MM, Yang K, Melick ER, et al. Patients undergoing recurrent CT scans: assessing the magnitude. Eur Radiol 2020;30(4):1828-1836.

[12] Miller GF, DePadilla L, Xu L. Costs of nonfatal traumatic brain injury in the United States, 2016. Med Care 2021;59(5):451-455.

[13] Alouani AT, Elfouly T. Traumatic brain injury (TBI) detection: past, present, and future. Biomedicines 2022;10(10):2472.

[14] Sheth KN, Mazurek MH, Yuen MM, et al. Assessment of brain injury using portable, low-field magnetic resonance imaging at the bedside of critically ill patients. JAMA Neurol 2021;78(1):41-47.

[15] Shahrestani S, Strickland BA, Bakhsheshian J, et al. Transcranial eddy current damping sensors for detection and imaging of hemorrhagic stroke: feasibility in benchtop experimentation. Neurosurg Focus 2021;51(1):E15.

[16] Lee SK, Hua Y. Theory and mitigation of motional eddy current in high-field eddy current shielding. J Appl Phys 2024;136(2):024504.

[17] Kimberly WT, Sorby-Adams AJ, Webb AG, et al. Brain imaging with portable low-field MRI. Nat Rev Bioeng 2023;1(9):617-630.

[18] Shahrestani S, Zada G, Chou TC, et al. Noninvasive transcranial classification of stroke using a portable eddy current damping sensor. Sci Rep 2021;11(1):10297.

[19] Shahrestani S, Zada G, Tai YC. Development of computational models for microtesla-level magnetic brain scanning: a novel avenue for device development. BMC Biomed Eng 2022; 4(1):1.

[20] Gabriel C, Peyman A, Grant EH, et al. Electrical conductivity of tissue at frequencies below 1 MHz. Phys Med Biol 2009;54(16):4863-4878.

[21] Zhang P, Ran Y, Han L, et al. Nanomaterial technologies for precision diagnosis and treatment of brain hemorrhage. Biomaterials 2025;321:123269.

[22] Simulating Irregular Shapes: How to Import Curve Data and Layout into Solids. Available from: https://cn.comsol.com/blogs/modeling-irregular-shapes-how-to-import-curve-data-and-loft-a-solid/

[23] Gabriel C, Gabriel S. Compilation of the dielectric properties of body tissues at RF and microwave frequencies. King's College, London, Department of Physics 1996.

[24] Shahrestani S, Wishart D, Han SMJ, et al. A systematic review of next-generation point-of-care stroke diagnostic technologies. Neurosurg Focus 2021;51(1):E11.